

Nitrogen Removal by Immobilized Anammox Sludge using PVA Gel as Biocarrier

TRAN THI HIEN HOA¹, LUONG NGOC KHANH¹, LIU ZHIJUN², TAKAO FUJII³,
JOSEPH D. ROUSE⁴, and KENJI FURUKAWA¹

¹Graduate School of Science and Technology, Kumamoto University
/2-39-1 Kurokami, Kumamoto 860-8555, Japan

²Dalian University of Technology/158-41, Zhongshan Road, Dalian 116012, China

³Department of Applied Life Science, Faculty of Biotechnology and Life Science, Sojo University
/4-22-1 Ikeda, Kumamoto 860-0082, Japan

⁴Kuraray Co., Ltd./1621 Sakazu, Kurashiki 710-8622, Japan

Abstract

The use of a biomass carrier is preferred for the cultivation of slowly growing anammox sludge. In this study, PVA gel was selected as a biomass carrier for anammox sludge and applied in a fluidized-bed reactor (FBR). A recycle pump was used to induce a flow rate of 6 - 7 l/min to maintain fluidized bed conditions. Both influent NH₄-N and NO₂-N concentrations were increased stepwise to 300 mg N/l. With hydraulic retention times (HRTs) from 16 h to 9 h in phase 1, NH₄-N and NO₂-N removal efficiencies were about 81% and 92%, respectively. With HRTs from 9 h to 4 h in phase 2, NH₄-N removal efficiency was 77% and NO₂-N removal efficiency was 89%. The removal rates of ammonium and total nitrogen in phase 1 increased up to 0.71 and 1.35 kg N/m³/d, respectively. Maximum removal rates of ammonium and total nitrogen in phase 2 increased quickly up to 1.5 and 3.0 kg N/m³/d, respectively. Ratios of T-N removal, NO₂-N removal, and NO₃-N production to NH₄-N removal during phase 1 were 1.91:1.12:0.22. These ratios during phase 2 were 1.96:1.18:0.21. The color of the PVA-gel beads changed from white to brownish red, which is consistent with anammox bacteria. By the Denaturing Gradient Gel Electrophoresis (DGGE) method, both KSU-1 and KU-2 anammox strains were detected with KSU-1 in dominance in the FBR process.

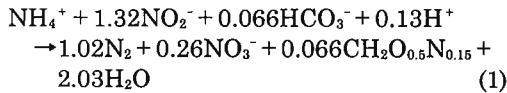
Key words: anammox, ammonium, fluidized-bed, FBR, nitrite, PVA-gel beads

INTRODUCTION

Ammonium pollution from sources such as food processing and agricultural industries is a growing concern to the water environment and as such has contributed to the increasing demand for more effective methods of nitrogen abatement. Traditionally, nitrogen removal from wastewater has been carried out by biological treatment involving the processes of autotrophic nitrification and heterotrophic denitrification. However, recently a newly discovered shortcut in the nitrogen cycle - Anaerobic Ammonium Oxidation (anammox)-

has been gaining much attention^{1, 2)}. For an ammonium-rich wastewater, when combined with a nitrification step this new process yields the formation of dinitrogen gas under anoxic conditions from the concomitant oxidation of ammonium and reduction of nitrite^{3, 4)}. This overall process requires only 50% of the oxygen needed for the traditional nitrification-denitrification method and, being fully autotrophic, no addition of organic carbon is needed⁵⁾. The anammox process is thus effective for nitrogen removal from wastewaters with low carbon content⁶⁾; in addition, sludge production is negligible⁶⁾,

thus making it an economically favorable treatment option. The stoichiometry of the anammox reaction has been determined to be⁷⁾:



A newly discovered anammox strain, KSU-1 (AB057453), was enriched from seed sludge of Kumamoto, Japan, and used in continuous-flow treatment with a fixed-bed attached-growth process⁹⁾. This KSU-1 strain had a 16S rDNA sequence similarity of 92.2% with archetypal *Candidatus* Brocadia anammoxidans (AJ131819) and considerably less sequence similarities to those of all other reported anammox planctomycetes⁹⁾. In a parallel study, using seed sludge from a distinctly different location in Japan, an anammox strain, KU-1 (AB054006), with a 99.1% sequence similarity to *B. anammoxidans*, was also identified⁵⁾ and used in continuous-flow treatment studies¹⁰⁾. The KU-2 (AB054007) strain, also enriched in Japan, had a very high sequence similarity with *Candidatus* Kuenenia stuttgartiensis (AJ250882)¹¹⁾.

Fluidized-bed reactors (FBRs) have been applied for denitrification and the anammox process was firstly discovered in a FBR⁴⁾. More recently, the FBR technology has been used for enrichment of anammox microorganisms⁶⁾ and other anammox treatment applications, thus confirming that FBR is well suited for the anammox process²⁾.

In this research, PVA-gel beads were used as biomass carriers for anammox sludge in a FBR. PVA-gel beads have a porous microstructure that allows for microorganisms to penetrate and colonize throughout the gel material, thus providing favorable conditions for retention and cultivation of slowly growing anaerobic microorganisms¹²⁾. In our laboratory, up-flow column reactors using a non-woven biomass carrier^{8, 10, 13)} and a packed-bed reactor using PVA-gel beads¹²⁾ have been well studied. These reactors, though, functioned in a semi plug-flow manner, thus much of the reactor volume was not effectively used due to either high nitrite concentration (more than 0.1 g N/l¹⁴⁾) near the inlet or very low substrate levels in other parts of the reactors.

Consequently, the new FBR was designed with the intent of reducing substrate inhibitions by thorough mixing using a high recycle flow rate. In addition, the PVA-gel beads maintain better contact with substrate under fluidized-bed conditions and nitrogen gas is more easily separated from the process. However, first attempts at using FBRs for anammox treatment have met with some difficulties and several cultivation attempts were hindered due to recycling pump failures⁷⁾. The objective of this research is to evaluate the ammonium removal capabilities of anammox sludge in a FBR using PVA-gel beads.

MATERIALS AND METHODS

FBR laboratory- scale system The total volume of the reactor used in this study was 4.06 liter and the liquid volume, consisting of reaction and clarification zones, was 3.55 liter. The reaction zone containing the carrier material had a diameter of 7.4 cm and height of 50 cm with a volume of 2.15 liter, which was used for determinations of hydraulic retention time (HRT). A schematic diagram of the FBR system is shown in Fig. 1. The reactor had an airtight cover with vents for gas collection, gas emission and thermostatic sensing. Nitrogen gas was collected by using gas sampling bag in phase 1 and a gas collector vessel in phase 2. Airtight integrity was maintained in the capped reactor by use of an effluent water trap. PVA-gel beads were fluidized in the reactor zone. In phase 2, a 80-ml precolumn containing seeded PVA-gel beads was installed to deplete dissolved oxygen from the influent.

Biocarrier material The PVA-gel beads have a diameter of 4 mm (Fig. 2a) with a solids content of about 10% and a specific gravity of 1.025¹⁵⁾ (Kuraray Co., Osaka, Japan), making them easy to suspend in water. They are hydrophilic in nature and have a porous structure with a continuum of passages 10 to 20 μm in throughout each bead^{12, 15)} (Fig. 2b)

Seed biomass The cultivated PVA-gel beads used for the fluidized bed reactor originated from a previously studies anammox

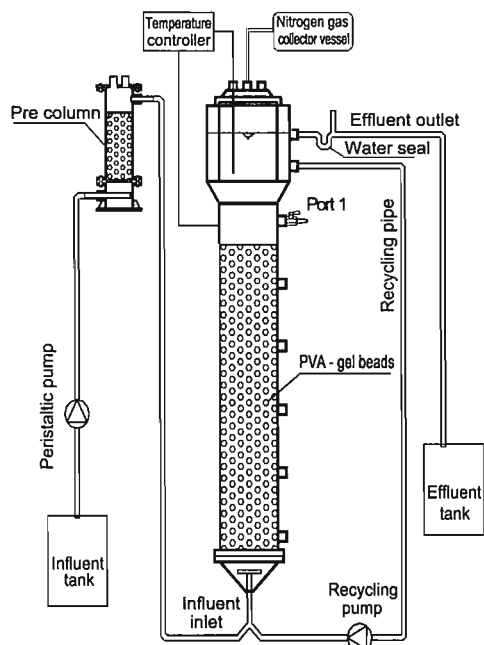


Fig. 1 Schematic diagram of FBR system used this study.

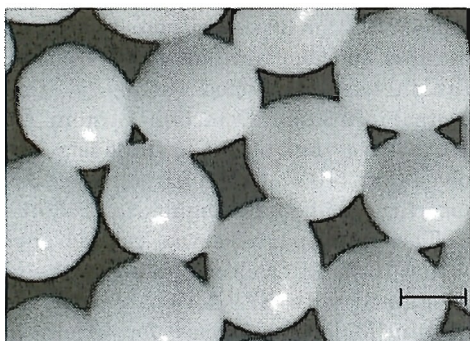


Fig. 2a Unused PVA-gel beads. Bar indicates 2 mm

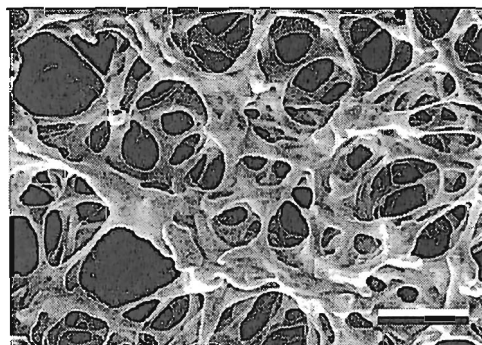


Fig. 2b Environmental scanning electron micrograph (ESEM) of the microstructure of an unused PVA-gel bead. Bar indicates 10 μm

packed-bed reactor. The total volume of PVA-gel beads was 0.8 l in phase 1 which included 0.7 l of cultivated PVA-gel beads and 0.1 l of new PVA-gel beads. In phase 2, 0.2 l of cultivated PVA-gel beads were added for a total PVA-gel volume of 1 l.

Synthetic wastewater Synthetic wastewater was prepared by adding ammonium and nitrite in the forms of $(\text{NH}_4)_2\text{SO}_4$ and NaNO_2 , respectively, to a mineral medium according to the composition given in Table 1. The influent wastewater was taken from the effluent of a 50-l non-woven anammox reactor over the first 120 days for quick start-up.

Operational conditions Influent was fed in up-flow mode using a peristaltic pump (Eyela Co., Ltd., Tokyo). Recycling condition was maintained by use of a magnetic drive pump (Iwaki Co., Ltd., Tokyo). The recycle flow rate was 360–420 l/h for a velocity of

Table 1 Composition of the synthetic wastewater

Composition	Concentration
$(\text{NH}_4)_2\text{SO}_4$ (mgN/l)	Variable (25–300)
NaNO_2 (mgN/l)	Variable (25–300)
KHCO_3 (mg/l)	125
KH_2PO_4 (mg/l)	54
$\text{FeSO}_4 \cdot 7\text{H}_2\text{O}$ (mg/l)	9
EDTA (mg/l)	5
Trace element solution I (mg/l): NaCl 500, KCl 700, $\text{CaCl}_2 \cdot 2\text{H}_2\text{O}$ 700, $\text{MgSO}_4 \cdot 7\text{H}_2\text{O}$ 500	2ml/l
Trace element solution II* (mg/l): $\text{CuSO}_4 \cdot 5\text{H}_2\text{O}$ 0.25, $\text{ZnSO}_4 \cdot 7\text{H}_2\text{O}$ 0.43, $\text{CoCl}_2 \cdot 6\text{H}_2\text{O}$ 0.24, $\text{MnCl}_2 \cdot 4\text{H}_2\text{O}$ 0.99, $\text{NaMoO}_4 \cdot 2\text{H}_2\text{O}$ 0.22, $\text{NiCl}_2 \cdot 6\text{H}_2\text{O}$ 0.19, NaSeO_4 0.11, H_3BO_3 0.014	1ml/l

*modified from⁶⁾

83.7~97.7 m/h to maintain fluidized bed conditions, which is comparable to velocities of 47 l/h or 12 m/h¹⁾, 255 l/h or 30~34 m/h⁴⁾, 45~65 m/h and 55 m/h¹⁶⁾, reported by others. The reactor temperature was maintained at 33°C to 35°C, controlled thermostatically with an external ribbon-heating element. A surface net was installed at the cone area to prevent PVA-gel beads from entering the recycle pipe and recycle pump. Light is known to have a negative effect (30~50% rate reduction) on ammonium removal rate⁶⁾; consequently, dark conditions were maintained using black vinyl sheet enclosures. Small styrafoam balls were placed in the feed storage tank to retard oxygen transfer to the synthetic wastewater. In addition, purging with nitrogen gas was used on a daily basis to keep dissolved oxygen levels in the influent below 0.5 mg/l.

Analytical methods Ammonium concentrations were measured by the phenate method using ortho-phenylphenol as a substitute for liquid phenol¹⁷⁾. In accordance with Standard Methods¹⁸⁾, nitrite concentrations were estimated by the colorimetric method and nitrate by the UV spectrophotometric screening method. Nitrite interferes with the nitrate UV screening method at 25% of the measured nitrate value on a nitrogen weight basis, thus nitrate results were corrected by calculation (i.e., the measured results of the nitrate screening assay were reduced by 25% of the results obtained by the nitrite colorimetric assay). Levels of pH were measured by using a Mettler Toledo-320 pH meter and DO was measured by using a DO meter (D-55, Horiba).

Denaturing Gradient Gel Electrophoresis (DGGE) Analysis DNA extraction and PCR amplification of 16S rDNA: DNA was extracted from anammox PVA sample using ISOIL (soil DNA extraction kit, NIPPON GENE). The 357F (5'-CCTACGGGAGGCAG CAG-3') and 534R (5'-ATTACCGCGGCTGC TGG-3') primers were used for amplification of 16S rDNA with 10ng DNA extracted. PCR amplification was carried out in 50 µl of reaction mixtures containing 1 µl of the extracted DNA, 10 pmol of each primer, 1µl

of KOD-plus (1 unit), 5 µl of 10X KOD buffer, 50 pM MgSO₄, 10 pM deoxynucleotide triphosphates (dNTPs) and 32 µl of sterile water. PCR was performed in a 2400 GeneAmp PCR System Thermal Cyclers (Perkin Elmer) consisting of an initial denaturation at 94°C for 2 min, followed by 27 cycles of 94°C for 15 s, 60°C for 30 s, 68°C for 30 s. The PCR-amplified 16S rDNA segments were electrophoresed on an agarose gels and excised fragments were purified using UltraClean DNA Purification Kit (MO BIO). For the second PCR amplification, the 357F + GC-clamp (5'-CGCCCGCCGCGCC CGCGCCCGTCCCGCCGCCCC CGCCCGCCT ACGGGAGGCAGCAG-3') and 534R (5'-ATTA CCGCGGCTGCT GG-3') primers were used with 30 ng purified DNA. Amplification mixtures had a final volume of 50 µl and contained 1 µl of the purified DNA, 5 pmol of each primer, 0.5 µl of KOD-plus (0.5 unit), 5 µl of 10X KOD buffer, 50 pM MgSO₄, 10 pM dNTPs and 32 µl of sterile water. Thermal cycling consisted of an initial denaturation at 94°C for 2 min, followed 9 cycles each of 94°C for 15 s, 60°C for 30 s, 68°C for 30 s.

Staining and photography of DGGE: DGGE analysis was conducted using a Dcode Universal Mutation Detection System (BIO RAD). Three µg of PCR products were resolved on 10% (w/v) acrylamide using denaturing gradients ranging from 30% to 65%. The electrophoresis was carried out at 100V for 16 h. After electrophoresis, the gels were stained with SYBR Gold Nucleic Acid Gel Stain (Molecular Probes) for 40 min and photographed with Fluorescent image analyzer (FUJIFILM).

RESULTS AND DISCUSSION

FBR start-up and performance Figure 3a shows the influent and effluent concentrations of nitrogenous compounds during the start-up phase, (phases 1 and 2), which lasted 120 days. Effluent from a 50-l nonwoven anammox reactor adjusted to desired levels of NH₄-N and NO₂-N was used as influent. Following 35 weeks of operation in phase 1, on day 365, a pre-column with 80 ml of cultivated PVA from a packed-bed reactor was installed to eliminate oxygen intrusion.

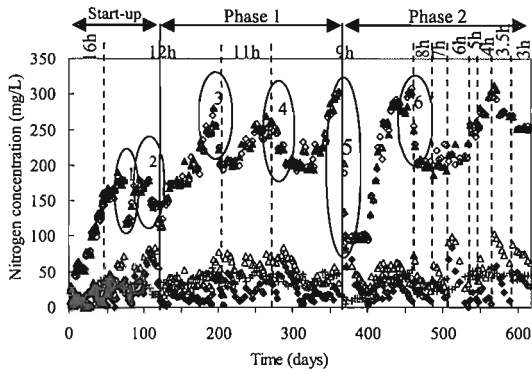


Fig. 3a Time courses of influent and effluent concentrations of nitrogenous compounds.
 Symbols: \blacktriangle Influent $\text{NH}_4\text{-N}$, \triangle Effluent $\text{NH}_4\text{-N}$,
 \diamond Influent $\text{NO}_2\text{-N}$, \blacklozenge Effluent $\text{NO}_2\text{-N}$,
 $+$ Effluent $\text{NO}_3\text{-N}$

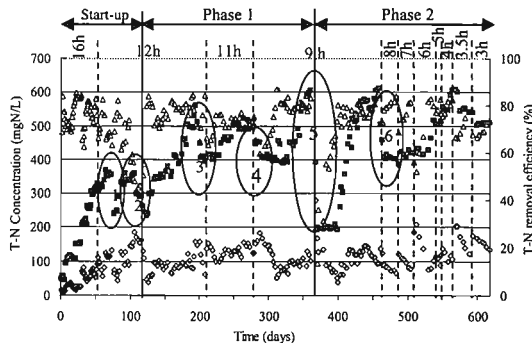


Fig. 3b Time courses of influent and effluent T-N concentrations and T-N removal efficiency.
 Symbols: \blacksquare Influent T-N, \diamond Effluent T-N,
 \triangle T-N Removal Efficiency

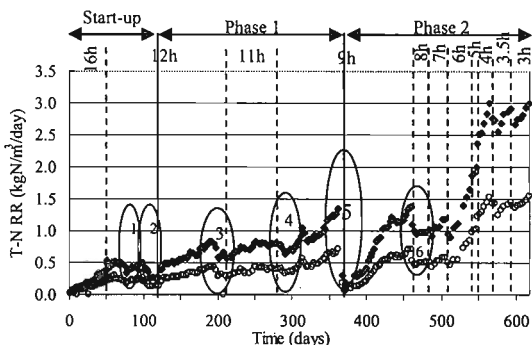


Fig. 3c Time courses of T-N and $\text{NH}_4\text{-N}$ removal rates.
 Symbols: \blacklozenge T-N Removal Rate,
 \circ $\text{NH}_4\text{-N}$ Removal Rate

At day 73 (Fig. 3a, circle 1), effluent concentrations of $\text{NH}_4\text{-N}$ and $\text{NO}_2\text{-N}$ were relatively high at about 70 and 40 mg N/l, respectively. This may have been due to the anammox bacteria having difficulty adapting to the increase in influent $\text{NH}_4\text{-N}$ and $\text{NO}_2\text{-N}$ levels of 175 mg N/l and the decrease in HRT from 16 to 12 h. Thus, influent $\text{NH}_4\text{-N}$ and $\text{NO}_2\text{-N}$ concentrations were both reduced to 120 mg N/l. At day 280 (circle 4), the HRT was further reduced from 11 to 9 h and influent $\text{NH}_4\text{-N}$ and $\text{NO}_2\text{-N}$ were decreased from 250 mg N/l to 200 mg N/l to avoid shock from overloading. Consequently, effluent concentrations of $\text{NH}_4\text{-N}$ and $\text{NO}_2\text{-N}$ decreased from about 84 mg N/l and 62 mg N/l (day 287) to 35 mg N/l and 9 mg N/l (day 309), respectively. In addition to offsets in loading patterns as indicated by circles 1 and 4 (see Figs. 3a, 3b and 3c), four other circles mark times when operational difficulties (pump failures, line breaks, etc.) resulted in adverse conditions that required immediate reductions in loading to allow for recuperation.

With an HRT of 16 h to 9 h in phase 1, the $\text{NH}_4\text{-N}$ removal efficiency was consistently about 81% and the $\text{NO}_2\text{-N}$ removal efficiency was about 92% ($n=73$). With an HRT of 9 h to 4 h in phase 2, $\text{NH}_4\text{-N}$ and $\text{NO}_2\text{-N}$ removal efficiencies were lower (ca. 77% and 89% ($n=59$), respectively). When the HRT was further reduced from 4 h to 3 h, $\text{NH}_4\text{-N}$ removal efficiency decreased to about 70%, with the $\text{NO}_2\text{-N}$ removal efficiency at about 86% ($n=13$). The effluent concentrations of $\text{NO}_3\text{-N}$ are shown in Table 2. These values were raised up stepwise except when adverse conditions occurred (as indicated by circles).

Figure 3b presents the influent and effluent T-N concentrations and T-N removal efficiencies in the three phases. Throughout phase 1 the T-N removal efficiency was about 77% ($n=73$) except during system upsets (circles 3 and 4). At day 361, with an HRT of 9 h, influent T-N was 606 mg/l and effluent T-N was 101 mg/l for a removal efficiency of 83%.

In phase 2 from day 365 to 564 (except during system upsets - circles 5 and 6), T-N removal efficiency was about 75% ($n=59$). At day 459, with an HRT of 9 h, influent T-N

was at its maximum value of 611 mg/l and effluent T-N was 94 mg/l and T-N removal efficiency was also at a maximum of 85%, which is almost same as the results on day 361 that were taken just before a major system failure (due to a broken recycle pump). These results show that the FBR had completely recovered over a 3-month period after being restarted (circle 5). Following day 564, with an HRT of 4 h, influent T-N was very high at 605 mg/l and effluent T-N was 106 mg/l for a removal efficiency of about

83%, which was maintained over the last 7 weeks of the study.

In phase 2 from day 565 to 617, T-N removal efficiency was about 70% (n=13) with influent T-N concentrations ranged between 550 and 500 mg/l. These data were lower than results in phase 1 and the initial period of phase 2. This observation may have been due to the short HRTs of 3.5 and 3 h. Generally, the HRTs of others studies were not less than 4 h (see Table 3).

T-N and NH₄-N removal rates are shown

Table 2 Effluent concentrations of NO₃-N and assessment of anammox activity

Phase	Period of time	Effluent concentration of NO ₃ -N (mg N/l)		Assessment of anammox activity	Note
		Positive activity	Negative activity*		
Start-up	Day 0-60	21.6 ± 11.4 (n=56)		+ Good	
	61-85		27.3 ± 4.6 (n=12)	- Bad	Circle 1
	86-98	31.4 ± 2.9 (n=6)		+ Good	
	99-120		22.1 ± 6.1 (n=10)	- Bad	Circle 2
1	121-192	38.4 ± 7.4 (n=29)		+ Good	
	193-216		36.8 ± 7.4 (n=9)	- Bad	Circle 3
	217-279	42.4 ± 4.9 (n=20)		+ Good	
	280-300		34.6 ± 4.2 (n=7)	- Bad	Circle 4
2	301-364	40.5 ± 6.3 (n=24)		+ Good	
	365-379		9.5 ± 3.8 (n=4)	-- very bad	Circle 5
	380-412	19.2 ± 7 (n=13)		+ recovering	
	413-459	43.1 ± 4.6 (n=20)		+ Good	
	460-470		24.4 ± 3.7 (n=5)	- Bad	Circle 6
	471-504	30.8 ± 5.8 (n=10)		+ Good	
	505-564	42.2 ± 8.9 (n=16)		+ + very good	
565-617	43.9 ± 3.1 (n=13)		+		

*negative activity was mentioned based on 6 circles mark times:

- circles 1 and 4: anammox bacteria having difficulty adapting to the increase in influent NH₄-N and NO₂-N levels and the decrease in HRT (hydraulic retention time)

- circles 2, 3, 5 and 6: operational difficulties (pump failures, line breaks, etc)

Table 3 Comparisons of anammox activities in this and other studies

Reactors	Carrier material	Influent NH ₄ -N concentration (kg NH ₄ -N/m ³)	Influent NO ₂ -N concentration (kg NO ₂ -N/m ³)	HRT* (hrs)	T-N removal rate (kg N/m ³ _{reactor} /d)	References
FBR, phase 1	PVA (3.5-4mm)	0.1-0.3	0.1-0.3	12~9	1.35	This study
FBR, phase 2	PVA (3.5-4mm)	0.1-0.3	0.1-0.3	9~3	2.99	This study
Denitrifying FBR (after the onset of anammox)	Sand particle (0.3-0.6 mm)	0.1-0.15	-	4.2	1.5	4)
FBR (synthetic WW)	Sand particle (0.3-0.6 mm)	0.07-0.84	0.07-0.84	22~42	1.8	1)
FBR (sludge digestion effluent)	Sand particle (0.3-0.6 mm)	0.07-0.84	1.1-2.1	3.5~264	1.5	1)
Fixed bed reactor	Glass beads (3-5mm)	0.07-0.84	0.07-0.84	6~23	1.1	1)
Packed-bed reactor	PVA (3.5-4mm)	0.025-0.35	0.025-0.35	6.460.7	1.92	12)

* Hydraulic retention time

in Fig. 3c. During the 244 days of phase 1, the T-N removal rate increased from 0.27 to 1.35 kg N/m³ reactor/d by increasing the influent T-N from 200 to 600 mg/l and influent flow rate from 4.3 l/d to 5.73 l/d. The NH₄-N removal rate was from 0.13 to 0.71 kg N/m³ reactor/d.

The highest T-N and NH₄-N removal rates obtained in this study of 3.0 kg N/m³ reactor/d and 1.5 kg N/m³ reactor/d, respectively, occurred during phase 2. In addition, during the last 53 days of the study (from day 565 to day 617), T-N and NH₄-N removal rates of 3.0 kg N/m³ reactor/d and 1.6 kg N/m³ reactor/d occurred when influent flow rates were higher with 15 and 17 l/d and, thus, HRTs were shorter at 3.5 h and 3 h. However, a T-N removal efficiency of 70% was obtained.

Table 3 represents comparison of anammox activities of this and other studies. The T-N removal rate during phase 1 of this study was lower than the values of studies of FBRs using sand particle as carrier material^{14, 16}. However, this value during phase 2 of this study was higher in comparison with the above studies. Therefore, the FBR in this study showed a high anammox activity for high strength ammonium wastewater.

In addition, the T-N removal rate of a fixed bed reactor using glass beads as a carrier material¹ was 1.1 kg N/m³ reactor/d and lower than in comparison with other FBRs' values. The T-N removal rate of the packed-bed reactor using PVA-gel beads¹² was higher than of the FBR using PVA-gel beads in phase 1 and lower than of FBR using PVA-

gel beads in phase 2. If the FBR using PVA-gel beads was not disturbed severely by mechanic problem in phase 1 (circle 5), anammox activity was not affected heavily and an equal or higher T-N removal rate in compare with T-N removal rate of the packed bed reactor may obtained. The pre-column was installed to deplete DO from the influent in phase 2 but not in phase 1. Therefore, T-N removal rate of phase 1 may be difficult to obtain an equal or higher than T-N removal rate of phase 2 even without any disturbance in phase 1. During phase 2, FBR was disturbed slightly by mechanical problem (circle 6), hence, the very high T-N removal rate of 3.0 kg N/m³ reactor/d was obtained.

Ratios of T-N removal, NO₂-N removal, and NO₃-N production to NH₄-N removal during phases 1 as shown in Fig. 4a were 1.91:1.12:0.22, respectively. These values are corroborative of the stoichiometry of the anammox reaction (Eq. 1). These same ratios during phase 2 of 1.96:1.18:0.21 (Fig. 4b) were improved (i.e., closer to the theoretical ratios) over the results obtained at phase 1. The above observations indicate that the T-N removal capacity during phase 2 was higher than during phase 1 with the same NH₄-N level. Consequently, the anammox activity at phase 2 was considered better than at phase 1.

The correlation between T-N removal and loading rates was generally linear (Fig. 5). With T-N loading rates were lower than 3.6 kg N/m³ reactor/d, average T-N removal efficiency obtained higher than 74%. However, with T-

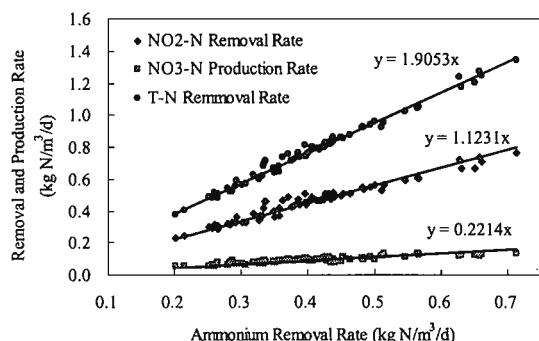


Fig. 4a T-N removal, NO₂-N removal and NO₃-N production with respect to NH₄-N removal in phase 1 (days 121-364)

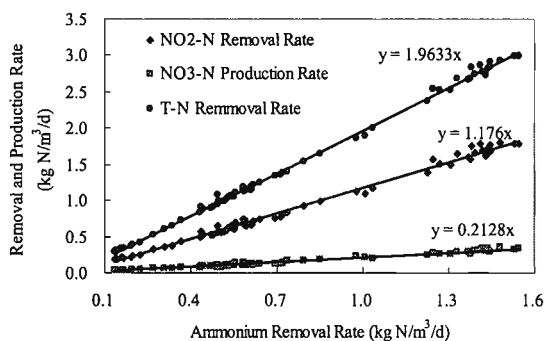


Fig. 4b T-N removal, NO₂-N removal and NO₃-N production with respect to NH₄-N removal in phase 2 (days 365-617)

N loading rates were higher than 3.6 kg N/m³ reactor/d, average T-N removal efficiency was lower than 74%. Therefore, T-N loading rate of 3.6 kg N/m³ reactor/d is recommended.

Gas production was measured over the last 200 days. In other studies for the anammox process, composition of the gas production was analyzed many times by gas chromatography and levels of N₂ in the off-gas were determined to be greater than 99.5% and nitrous oxide was below detection¹³⁾, thus the gas produced in this study is assumed to result from T-N removal in keeping with the anammox reaction (Eq. 1). The trend in gas production rate closely followed the T-N removal rate as shown in Fig. 6. When the T-N removal rate was 3.0 kg N/m³ reactor/d on day 564, gas production rate was at its maximum of 6.2 l/d. Figure 7 shows the correlation between gas production and T-N removal rate (n=71). The observed ratio of gas production (l/d) to T-N removal (kg N/m³ reactor/d) (1.91, slope of the observed production plot in Fig. 7) was not significantly different from the theoretical ratio (1.94, slope of the theoretical production plot in Fig. 7) with a 97% confidence interval.

Other observations Table 4 shows the maximum PVA loading rate in packed-bed reactor and FBR. The maximum PVA loading rate was calculated by Eq. 2 as follow:

$$\max PVA LR = \frac{(\max T-N RR) \times V_{reactor}}{V_{PVA}} \quad (2)$$

Where:

- max PVA LR: the maximum PVA loading rate
- max T-N RR: the maximum T-N removal rates of the packed-bed reactor and FBR
- V_{reactor}: the volumes of packed-bed reactor and FBR

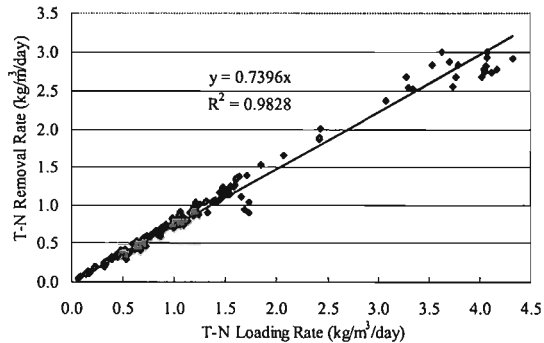


Fig. 5 Correlation between T-N removal rate and T-N loading rate (617 days)

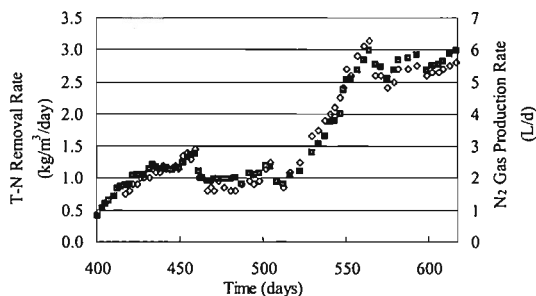


Fig. 6 Time courses of T-N removal rates and observed gas production rate
■ T-N Removal Rate, ◇ N₂ gas production

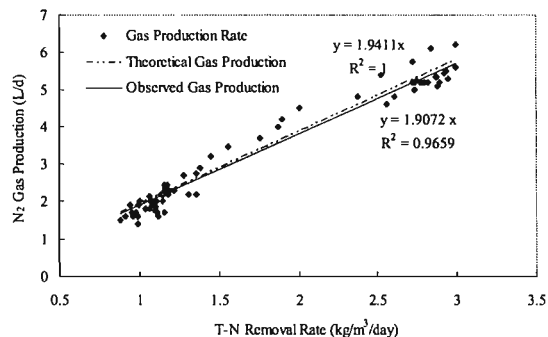


Fig. 7 Observed gas production rate as a function of T-N removal rate. The theoretical gas production is based on the ideal gas law assuming N₂ production in accordance with the anammox reaction

Table 4 Maximum PVA loading rate in packed-bed reactor and FBR (calculated by T-N removal rate based on volume of PVA-gel beads)

Parameters	Packed-bed reactor using PVA-gel beads	FBR using PVA-gel beads (phase 1)	FBR using PVA-gel beads (phase 2)
Volume of PVA-gel beads (l)	0.6	0.8	1
PVA loading rate (kg N/m ³ PVA/d)	3.84	3.63	6.43

- V_{PVA} : the settled-bed volumes of PVA-gel beads in the packed-bed reactor and FBR

The settled-bed volumes of PVA-gel beads in the packed-bed reactor and FBR during phases 1 and 2 were 0.6 l, 0.8 l and 1 l, respectively. The PVA loading rate of the FBR during phase 1 was lower than that of the packed-bed reactor because of the system disturbance (circle 5) as mention above. In phase 2, the maximum PVA loading rate was at its highest of 6.4 kg N/m³_{PVA}/d. This promising value shows good agreement for high nitrogen removal processes from wastewater without necessity of a large volume of PVA-gel beads.

During phase 1, the influent pH was about 7.9 (n=42) without adjustment and the pH at port 1 (end of reaction zone) was 8.3 (n=42), which was significantly higher than the influent value and in keeping with chemistry of anammox reaction, i.e., consumption of acidity results in pH increase in the anammox process (Eq. 1). In phase 2, the influent pH was about 7.5 (n=72) without adjustment and pH at port 1 was 8.0 (n=72), which was also significantly higher than the influent level.

Microscopic observations As indicated in Fig. 8, the color of the surface of the PVA-gel beads change from white to a brownish red color which is specific for anammox bacteria. However, anammox bacteria could not penetrate significantly inside the PVA-gel beads during 6 months. In addition, following 15 months, the anammox bacteria were observed only in the outer 1 mm of surface of the beads. This may have been due to the bacteria forming a tight layer at the outer surface. Therefore, anammox bacteria could not penetrate into the center of the beads despite the diameter of pores in the center being larger than in the outer surface (20 μ m versus 10 μ m, respectively). Furthermore, nutrient consumption across the outer surfaces of the beads was also a possible reason. These observations were also similar in the packed-bed reactor¹²⁾.

Denaturing Gradient Gel Electrophoresis At day 564, anammox sludge on PVA-

gel beads was sampled to identify gene by using the DGGE method. Both KSU-1 and KU-2 were present in the sample; however, KSU-1 was dominant as shown in Fig. 9. This may have been due to the cultivated PVA-gel beads of the FBR originating from the packed-bed reactor of which only the KSU-1 strain was detectable following one year of continuous anammox treatment in packed-bed reactor¹²⁾.

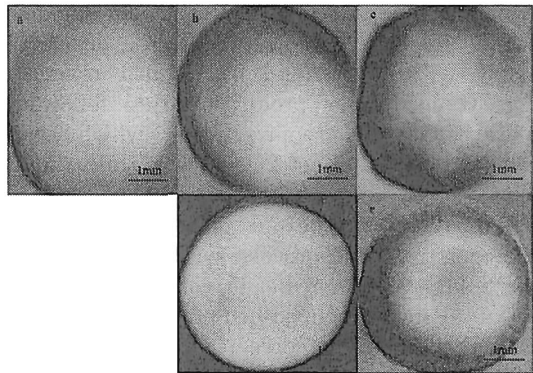


Fig. 8 PVA-gel beads before and after use in FBR.
a. New PVA-gel beads.
b. PVA-gel beads after 6 months
c. PVA-gel beads after 15 months
d. Center of PVA-gel beads after 6 months
e. Center of PVA-gel beads after 15 months

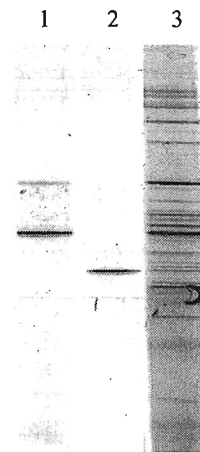


Fig. 9 DGGE of PCR products from anammox biomass in PVA-gel beads
Lane 1: KSU-1 Marker
Lane 2: KU-2 Marker
Lane 3: anammox sludge in PVA-gel beads

CONCLUSIONS

At HRTs between 9 to 4 h, T-N removal efficiency was maintained at about 75% or greater during phase 2 of this study. In addition, at an HRT of 4 h with an influent T-N of 605 mg/l a removal efficiency of 83% was achieved. However, T-N removal efficiency decreased to 70% when the HRT was reduced from 4 h to 3 h. T-N removal rates reached as high as 1.35 kg N/m³ reactor/d (NH₄-N removal rate, 0.71 kg N/m³ reactor/d) in phase 1 and 3.0 kg N/m³ reactor/d (NH₄-N removal rate, 1.5 kg N/m³ reactor/d) in phase 2, which is superior to a T-N removal rate of about 2 kg N/m³ reactor/d observed in a previous study with a PVA-gel packed-bed reactor. The trend in gas production rate followed closely the T-N removal rate, which was followed over the last 200 days of this study. The use of PVA gel in a FBR was thus demonstrated to be an effective high-rate nitrogen removal process without the need for a large PVA-gel beads volume as would be used in a packed-bed reactor. By the DGGE method, the presence of both KSU-1 (AB057453) and KU-2 (AB054007) anammox strains were confirmed in the FBR with KSU-1 greatly in dominance.

REFERENCES

- 1) Strous, M., van Gerven, E., Zheng, P., Kuenen, J.G., and Jetten, M.S.M.: Ammonium removal from concentrated waste streams with the anaerobic ammonium oxidation (Anammox) process in different reactor configurations, *Wat. Res.*, 31, 1955-1962 (1997)
- 2) Strous, M., van Gerven, E., Kuenen, J.G., and Jetten M.S.M.: Effects of aerobic and micro-aerobic conditions on anaerobic ammonium oxidizing (anammox) sludge, *Appl. Environ. Microbiol.*, 63, 2446-2448 (1997)
- 3) Mulder, A., van de Graaf, A.A., Robertson, L.A., and Kuenen, J.G.: Anaerobic ammonium oxidation discovered in a denitrifying fluidized bed reactor, *FEMS Microbiol. Ecol.*, 16, 177-184 (1995)
- 4) Strous, M., Fuerst, J.A., Kramer, E.H.M., Logemann, S., Muyzer, G., van de Paschoonen, K.T., Webb, R., Kuenen, J.G., and Jetten, M.S.M.: Missing lithotroph identified as new planctomycete, *Nature*, 400, 446-449 (1999)
- 5) Fux, C., Bohler, M., Huber, P., Brunner, I., and Siegrist, H.: Biological treatment of ammonium-rich wastewater by partial nitrification and subsequent anaerobic ammonium oxidation (anammox) in a pilot plant, *J. Biotechnol.*, 99, 295-306 (2002)
- 6) van de Graaf, A.A., de Bruijn, P., Robertson, L.A., Jetten, M.S.M., and Kuenen, J. G.: Autotrophic growth of anaerobic ammonium-oxidizing microorganisms in a fluidized bed reactor, *Microbiology*, 142, 2187-2196 (1996)
- 7) Strous, M., Heijnen, J.J., Kuenen, J.G., and Jetten, M.S.M.: The sequencing batch reactor as a powerful tool for the study of slowly growing anaerobic ammonium-oxidizing microorganisms, *Appl. Microbiol. Biotechnol.*, 50, 589 - 596 (1998)
- 8) Furukawa, K., Rouse, J.D., Yoshida, N., and Hatanaka, H.: Mass cultivation of anaerobic ammonium-oxidizing sludge using a novel nonwoven biomass carrier, *J. Chem. Eng. Jpn.*, 36, 1163-1169 (2003)
- 9) Fujii, T., Sugino, H., Rouse, J.D., and Furukawa, K.: Characterization of the microbial community in an anaerobic ammonium-oxidizing biofilm cultured on a nonwoven biomass carrier, *J. Biosci. Bioeng.*, 94, 412-418 (2002)
- 10) Rouse, J.D., Yoshida, N., Hatanaka, H., Imajo, U., and Furukawa, K.: Continuous treatment studies of anaerobic oxidation of ammonium using a nonwoven biomass carrier, *Jpn. J. Wat. Treat. Biol.*, 39, 33-41 (2003)
- 11) Imajo, U., Ishida, H., Fujii, T., Sugino, H., Rouse, J.D., and Furukawa, K.: Genbank direct submission. AB054007 (uncultured anoxic sludge bacterium KU2) (2001)
- 12) Rouse, J.D., Fujii, T., Sugino, H., Tran, H., and Furukawa K.: PVA-gel beads as a biomass carrier for anaerobic oxidation of ammonium in a packed-bed reactor, CD-ROM. In Proceedings of 5th International Exhibition and Conference on Environmental Technology. Heleco '05 (2005) http://library.tee.gr/digital/m2045/m2045_rouse.pdf

- 13) **Furukawa, K., Rouse, J.D., Imajo, U., Nakamura, K., and Ishida, H.:** Anaerobic oxidation of ammonium confirmed in continuous flow treatment using a novel nonwoven biomass carrier, *Jpn. J. Wat. Treat. Biol.*, 38, 87-94 (2002)
- 14) **Strous, M., Kuenen, J.G., and Jetten, M.S.M.:** Key physiology of anaerobic ammonium oxidation, *Appl. Environ. Microbiol.*, 65, 3248-3250 (1999)
- 15) <http://www.kuraray-efd.com/kuragel/>
- 16) **Rabah, F.K.J. and Dahab, M.F.:** Biofilm and biomass characteristics in high-performance fluidized-bed biofilm reactors, *Wat. Res.*, 38, 4262-4270 (2004)
- 17) **Kanda J.:** Determination of ammonium in seawater based on the indophenol reaction with o-phenylphenol (OPP), *Wat. Res.*, 29, 2746-2750 (1995)
- 18) **APHA, AWWA, WPCF:** Standard Methods for the Examination of Water and Wastewater, 19th edition, American Public Health Association, Washington, D.C. (1995)

(Submitted 2006. 4. 20)

(Accepted 2006. 6. 20)